Anastasios Petrou[a], Panagiotis Pergantis[a], Gregor Ochsner, Raffael Amacher, Thomas Krabatsch, Volkmar Falk, Mirko Meboldt and Marianne Schmid Daners*

Response of a physiological controller for ventricular assist devices during acute patho-physiological events: an *in vitro* study

DOI 10.1515/bmt-2016-0155
Received July 12, 2016; accepted January 5, 2017; online first February 9, 2017

Abstract: The current paper analyzes the performance of a physiological controller for turbodynamic ventricular assist devices (tVADs) during acute patho-physiological events. The numerical model of the human blood circulation implemented on our hybrid mock circulation was extended in order to simulate the Valsalva maneuver (VM) and premature ventricular contractions (PVCs). The performance of an end-diastolic volume (EDV)-based physiological controller for VADs, named preload responsive speed (PRS) controller was evaluated under VM and PVCs. A slow and a fast response of the PRS controller were implemented by using a 3 s moving window, and a beat-to-beat method, respectively, to extract the EDV index. The hemodynamics of a pathological circulation, assisted by a tVAD controlled by the PRS controller were analyzed and compared with a constant speed support case. The results show that the PRS controller prevented suction during the VM with both methods, while with constant speed, this was not the case. On the other hand, the pump flow reduction with the PRS controller led to low aortic pressure, while it remained physiological with the constant speed control. Pump backflow was increased when the moving window was used but it avoided sudden undesirable speed changes, which occurred during PVCs with the beat-to-beat method. In a possible clinical implementation of any physiological controller, the desired performance during frequent clinical acute scenarios should be considered.

Keywords: physiological control; premature ventricular contraction (PVC); suction; Valsalva maneuver (VM); ventricular assist device (VAD); volume measurement.

Introduction

Implantable ventricular assist devices (VADs) have become a viable solution for the ever growing population of heart failure patients. The continually improving clinical outcome of the VAD-therapy [28] play an important role on this result. According to data presented in [12], which was derived from more than 15,000 patients, the 1 year and 2 year survival rates with turbodynamic VADs (tVADs) currently reach 80% and 70%, respectively, while the quality of life remains improved after 2 years compared to pre-implantation. More than 90% of the VAD patients receive a tVAD. Although a reduction of adverse events has been reported during the last few years, complications of this therapy such as hemolysis, cardiac arrhythmias, pump thrombosis, gastrointestinal bleeding, right ventricular (RV) failure and left ventricular (LV) overloading, still pose a problem. Despite the increased durability of newer generation of pumps, a stable incidence of device malfunction and exchange due to all causes is evident [12, 34].

Several research groups [1, 3, 6, 15, 21, 22, 26, 33] have proposed physiological control as a solution to reduce or even eliminate overpumping and underpumping events, which are presumably related to adverse events, such as hemolysis, pump thrombosis and RV failure. These control strategies are based on various signals, such as the LV pressure (LVP), the LV volume (LVV), the aortic pressure

[a]These authors contributed equally to the study.
***Corresponding author: Marianne Schmid Daners,** pd|z Product Development Group Zurich, Department of Mechanical and Process Engineering, ETH Zurich, CLA G21.1 Tannenstr. 3, 8092 Zurich, Switzerland, Phone: + 41 44 632 2447, E-mail: marischm@ethz.ch
Anastasios Petrou and Mirko Meboldt: pd|z Product Development Group Zurich, Department of Mechanical and Process Engineering, ETH Zurich, 8092 Zurich, Switzerland
Panagiotis Pergantis, Thomas Krabatsch and Volkmar Falk: German Heart Institute Berlin, Department of Cardiothoracic and Vascular Surgery, Augustenburger Platz 1, 13353 Berlin, Germany
Gregor Ochsner: pd|z Product Development Group Zurich, Department of Mechanical and Process Engineering, ETH Zurich, 8092 Zurich, Switzerland; and Institute for Dynamic Systems and Control, Department of Mechanical and Process Engineering, ETH Zurich, 8092 Zurich, Switzerland
Raffael Amacher: Wyss Translational Center Zurich, ETH Zurich, 8092 Zurich, Switzerland

(AoP), or the pump flow. Their goal is to adjust the speed and ultimately the blood flow of a tVAD such that the resulting cardiac output (CO) meets the perfusion requirements of the circulation. By matching the pump flow to the hemodynamic status of the patient, adverse events related to overpumping and underpumping can be prevented and the physiological adaptation of the CO is restored.

All physiological controllers extract one or more indices from either a measured or an estimated signal of the heart-tVAD system. These indices are fed into a control system which adjusts the desired speed of the tVAD. In [21, 22] the authors implemented a beat-to-beat extraction algorithm for their control indices, namely the end-diastolic pressure (EDP) and mean pump flow, respectively. In [3, 6, 26, 33] the authors proposed signal processing algorithms, which extract the indices of the end-diastolic volume (EDV), the pump pressure difference, the pump speed pulse, or the EDP over a time window with a predefined fixed length. Particularly, in [26] and [6] a moving window with a length of 3 s of the measured signals was implemented in order to extract their respective control inputs, whereas Wang et al. [33] proposed a moving 1 s time window. The suction detection algorithm developed in [3] uses a moving maximum search algorithm for the identification of the diastolic level of the pulsation of the pump differential pressure. Additionally, authors in [9] used low-pass filtering methods, such as the non-linear morphological filter, in order to feed their controller with the required mean pump flow.

The controller presented in [26] was evaluated by *in vitro* experiments, which represent wide-range variations of cardiovascular parameters and simulate resting or exercising conditions. Similar experiments for testing physiological controllers either *in silico* or *in vitro* are presented in [3, 15, 21, 23]. In contrast, authors in [18] investigated the response of several physiological controllers during more sudden changes in hemodynamic parameters. These changes were related to exercise (CO increase) and head-up tilt (CO decrease), simulated through a detailed numerical model [16]. Additional cases that lead to such sudden changes are related to patho-physiological events such as respiration (deep expiration or inspiration), strain (Valsalva or Mueller maneuver, coughing or heavy lifting) or arrhythmia.

Approaches to simulate such patho-physiological events either numerically or by manipulating mechanical components have been proposed. In [17], the authors presented a numerical model of a human circulation that incorporates the influence of the intra-thoracic pressure (ITP) and can therefore potentially simulate respiration and the Valsalva maneuver (VM). However, the simulation of these events and their use for evaluating physiological controllers was not in the scope of their study. A study focused on VM simulation has been presented in [14], however without investigating a VAD-assisted circulation. In [32], the authors simulated VM in their mock circulation loop (MCL), which is built for evaluating bi-ventricular assist devices (BiVADs). They were able to reproduce VM by manipulating the mechanical valves of their MCL, which represented the systemic and pulmonary vascular resistances, in order to apply a resistance increase, thereby emulating the influence of an increase of the ITP. These simulations were later used to evaluate physiological controllers for BiVAD support cases [30]. Amacher et al. [2] simulated premature ventricular contractions (PVCs) in order to evaluate arrhythmia detection algorithms, when a pulsatile speed mode of a tVAD, synchronized to the heart cycle, was implemented.

The current paper describes how our numerical model of the human blood circulation [24] was extended to simulate specific patho-physiological events, namely PVCs and VM, by manipulating the heart rate (HR) and the ITP. For both extensions, we focused on the hemodynamics in the LV of a pathological circulation assisted by a tVAD, which was either controlled by one of several configurations of the preload responsive speed (PRS) controller [26] or set at a constant speed. The core algorithm of the PRS controller remained unchanged, but the EDV extraction algorithm was modified to influence the aggressiveness of the controller. The pros and cons of fast and slow response during PVCs and VM were analyzed and compared to the clinical case of the constant speed control. The potential of the proposed extended human blood circulation model for testing new control algorithms is indicated and possible complications of standalone physiological controllers discussed. The need for additional algorithmic features that will support the core of the physiological controller is highlighted to guarantee preventing undesired overpumping and underpumping events.

Materials and methods

Hybrid mock circulation

We conducted experiments on a hybrid mock circulation (HMC) based on the hardware-in-the-loop concept, which has been developed in our group [24]. Figure 1 shows a picture of the hardware part of the HMC, while its caption defines the parts and their manufacturer. In our experiments, a non-implantable mixed-flow turbodynamic blood pump that allows implementing various control approaches substituted the tVAD (c). The pump is connected to two pressure-controlled reservoirs (a), (b) and a back flow pump (d) ensures that the fluid level in the two reservoirs remains constant during the experiments.

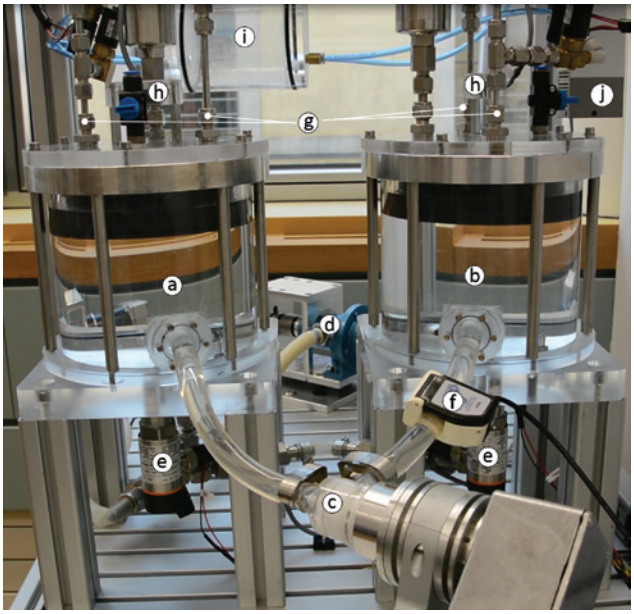

Figure 1: Picture of the hardware part of our hybrid mock circulation consisting of two pressure-controlled reservoirs (a) and (b), a blood pump head (Deltastream DP2, Xenios AG, Heilbronn, Germany) (c) equipped with an encoder (ME22, PWB Encoders GmbH, Eisenach, Germany) and an industrial motor controller (Accelus, ASP-090-09, Copley Controls Corp., Canton, MA, USA), a backflow pump (Moyno 500 Pumps-200 Series, Moyno, Inc., Springfield, OH, USA) (d), two fluid-pressure sensors (PN2009, IFM Electronic GmbH, Essen, Germany) (e), one ultrasonic flow probe (TS410/ME-11PXL, Transonic Systems, Inc., Ithaca, NY, USA) (f), one proportional solenoid inlet valve (PVQ33-5G-23-01F, SMC Pneumatics, Tokyo, Japan) and two proportional solenoid outlet valves (PVQ33-5G-40-01F, SMC Pneumatics,Tokyo, Japan) per reservoir (g), two fluid-level sensors (GP 2Y0D810Z0F, Sharp, Osaka, Japan) (h), a vacuum receiver (i) and a vacuum pump (ZL112-K15LOUT-E26L-Q, SMC Pneumatics, Tokyo, Japan) (j).

The fluid level is measured by infrared range finders (h) and fed to the back flow pump-controller. The pressure in each reservoir is controlled using one proportional solenoid inlet valve and two proportional solenoid outlet valves (g) per reservoir, a vacuum receiver (i) and a vacuum pump (j), and one fluid-pressure (e) sensor per reservoir.

The reference signals for the pressure controllers of the two reservoirs are computed in real-time by a validated numerical model of the human blood circulation [7], based on the measured pump flow (f). This numerical model consists of lumped-parameter elements. Thus, the veins of the upper and lower limb circulation, the inferior vena cava, etc. are implemented with one classic Windkessel model, which does not allow an implementation of the ITP on the vessels and organs of the thorax separately. Therefore, the numerical model was extended for the current investigation as described below.

Hemodynamic influence of intrathoracic pressure variations and arrhythmia

In order to define the required modifications of the existing numerical model, the hemodynamic influence of ITP variations and PVCs had to be identified. For this purpose, the response of both a physiological and a pathological circulation during these events was analyzed based on clinical studies and is presented below.

The VM causes an increase in the ITP without hyperinflation of the lungs. In the physiological circulation, increased ITP causes a decrease in the RV preload and RV filling, leading to a decrease in LV preload and CO. In the pathological circulation, the decrease of CO is significantly smaller or even inverted compared to the healthy heart. That happens due to the blood pooling in the pulmonary vascular system which can compensate the decrease in the LV preload, thus preserving the LV EDV. The preserved LV EDV, in combination with the decrease in the LV afterload in the failing heart, is responsible for the altered influence of VM on CO and AoP in heart failure [20, 27, 29]. Similar ITP changes are observed during coughing, strain, bowel movement, heavy lifting etc. [20].

Arrhythmias cause abrupt changes in the CO. Bradycardia causes a decrease in the CO and an overload of the cardiopulmonary system. Tachycardia, both ventricular and supraventricular, impairs the diastolic filling of the ventricles, leading to a decrease of the CO. Extrasystoles cause a decrease in both LV and RV EDV by generating PVCs and disrupting the diastolic phase. Arrhythmias in the setting of left VAD therapy can lead to suction events because of a decrease in LV preload, for instance during bradycardia or tachycardia, leading to a reduction of the RV SV or directly in LV EDV during extrasystoles [27].

Extension of the numerical model

The numerical model has already been extended in order to emulate suction [25]. For the current study, we further extended it in order to account for the influences of ITP variations, based on the analysis presented above. Figure 2 shows the structure of the extended model. The systemic venous and arterial systems are now divided into an intrathoracic and an extrathoracic part. The resistance of the intrathoracic and extrathoracic veins, namely $R_{sv,it}$ and $R_{sv,et}$, respectively, are used to simulate the collapse of the large vessels when the transmural pressure is negative. Furthermore, we added a venous valve in order to prevent regurgitation of the venous return [11]. The ITP is implemented by adding its value to all pressure values inside the thoracic cavity. Table 1 lists the values of all new parameters introduced into the extended model as well as their source. The remaining parameters used in the model were the same as presented in [7].

Simulation of the Valsalva maneuver

Figure 3A and C show the input signals to simulate the VM. The ITP was increased manually by 30 mm Hg at $t \in (5, 15)$ s, and the HR varied according to clinical data presented in [14]. The amplitude of the ITP for the VM was defined such that the resulting AoP waveform matched those presented in clinical studies [11, 14, 29, 31].

Simulation of arrhythmia

Figure 3B and D show the input signals to simulate arrhythmia. We introduced several PVCs, as they were defined in [2]. For that, we altered the cardiac cycle of the time-varying elastance model of the simulated ventricles and atria. Soon after the end of the systole,

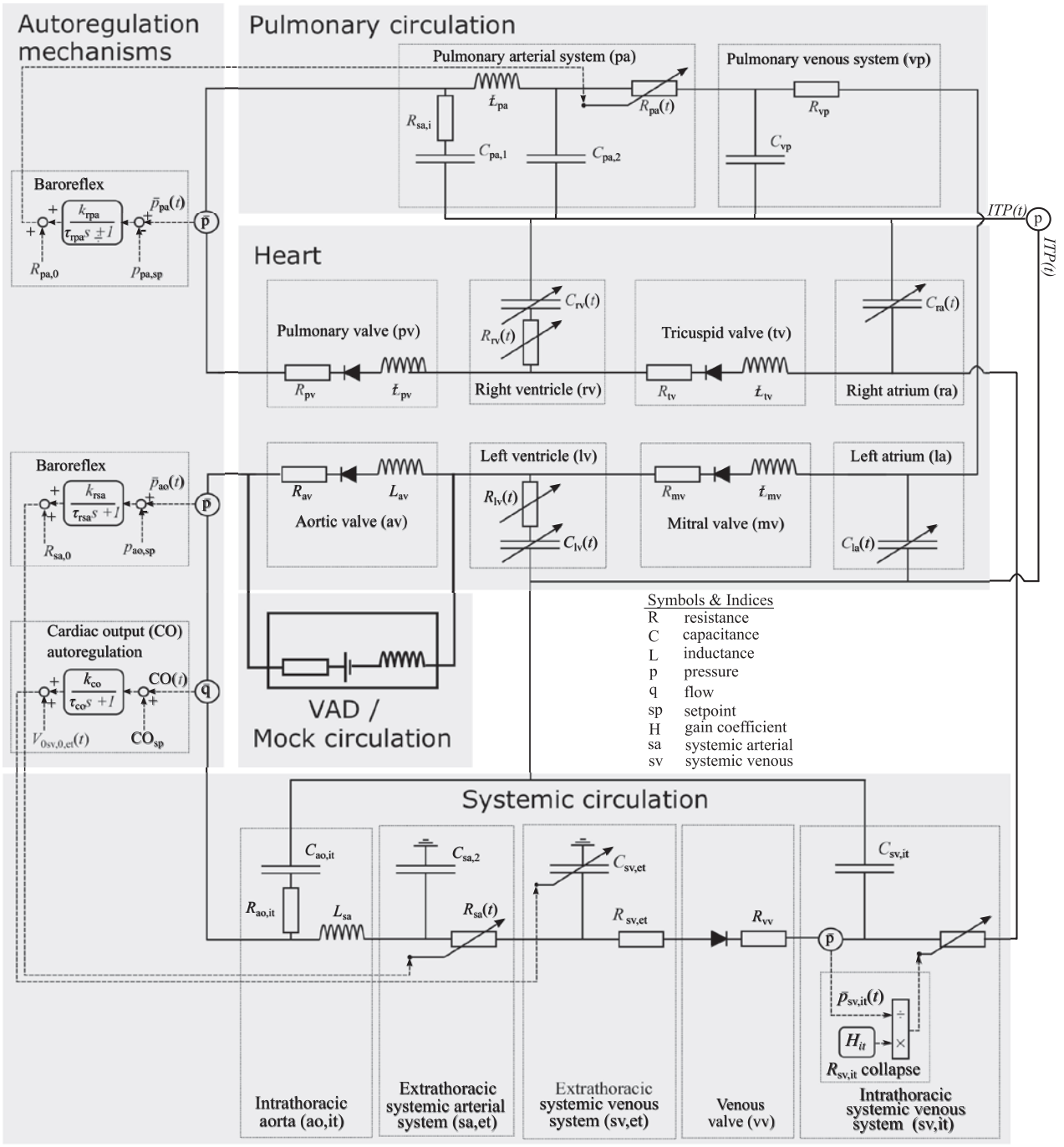

Figure 2: Electrical analog of the extended numerical model of the human blood circulation to include the influence of the intrathoracic pressure (ITP) on the organs of the thoracic cavity.
The systemic arterial and venous systems each consist of an intrathoracic and an extrathoracic part.

another ventricular contraction is triggered, while the subsequent diastolic phase is prolonged.

Experiments

For the physiological circulation, the HR was fixed at 70 bpm and increased up to 90 bpm during the VM event. The pathological circulation was simulated by decreasing the contractility of the LV to 34% of physiological contractility and increasing the HR to 90 bpm. For each experiment we ran the HMC until steady state was reached and then started either the VM or the PVCs experiment as depicted in Figure 3. The numerical model was executed with Matlab/Simulink running Real-Time Windows Target (The Mathworks Inc., Natick, MA, USA) and all signals were recorded at 1 kHz. A glycerol water mixture with viscosity of 2.8 mPa·s was used for all the experiments.

Table 1: Numbers and references used for the extended numerical model of the human blood circulation.

Parameter	Description	Value	Units	References
$V_{0sv,0,et}(t)$	Extrathoracic unstressed venous volume	3088	ml	[5, 24]
$V_{0sv,0,it}$	Intrathoracic unstressed venous volume	162	ml	[5, 24]
$C_{sv,et}$	Extrathoracic venous system compliance	55	ml/mm Hg	[14]
$C_{sv,it}$	Intrathoracic venous system compliance	10	ml/mm Hg	[14]
H_{it}	Intrathoracic vena cava collapse gain coefficient	0.547	mm Hg^2·s/ml	[7]

The extrathoracic unstressed venous volume is a variable input, all other parameters are constant.

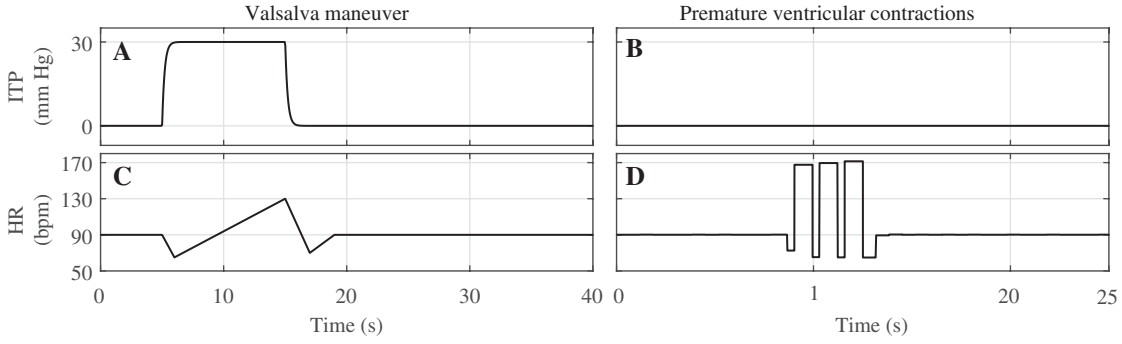

Figure 3: Defined values for the parameters that were varied during the experiments.
Panels (A) and (C) show the variation of the intrathoracic pressure (ITP) and the heart rate (HR) during the Valsalva maneuver (VM). Panels (B) and (D) show the ITP and the HR during the implementation of premature ventricular contractions.

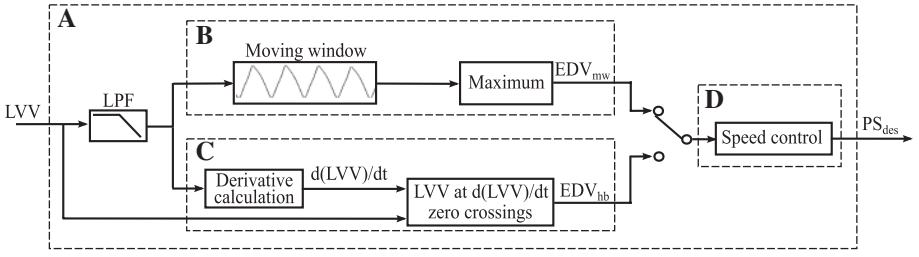

Figure 4: Structure of the PRS controller configurations of the tVAD (A).
The left ventricular volume (LVV) is processed and the end-diastolic volume is extracted either from the maximum of a moving window (EDVmw) (B) or at every heartbeat (EDVhb) (C). The extracted EDV is fed to the preload responsive speed (PRS) controller algorithm, which computes the desired pump speed (PSdes). The detailed structure of (D) is presented in [26].

Pump control configurations

Three different control configurations (C1–C3) of a tVAD were tested, as described below. The input to the PRS controller was the simulated LVV signal; the output was the desired pump speed (Figure 4A).

1) Constant speed (C1)
   For the C1 configuration, the PRS controller was disabled and the tVAD was operated at a constant speed. The speed was set to 4100 rpm, which yielded a CO of 5 l/min at rest.
2) Nominal PRS controller (C2)
   For the C2 configuration, we used the PRS controller as presented in [26], i.e. with a sliding window (Figure 4B) of 3 s to extract the EDV value. The lower limit for the pump speed was set to 1800 rpm.
3) Modified PRS controller with beat-to-beat EDV detection algorithm (C3)
   For the C3 configuration, we modified the signal-processing algorithm of the nominal PRS controller in order to extract the EDV value at every heartbeat. Figure 4C depicts the structure of the beat-to-beat EDV extraction algorithm. First, the simulated LVV signal is low-pass filtered with a second-order IIR filter with a cut-off frequency of 2.5 Hz. Second, the derivative of the signal is computed. When the derivative of the LVV signal changes sign the LVV signal is at a maximum, which corresponds to the EDV. Due to the continuous flow of a tVAD, no isovolumetric contraction occurs and the LVV signal has one distinct maximum. Therefore, the zero detection of the LVV derivative works reliably *in vitro*. The PRS controller structure (Figure 4D) remained unchanged, as presented in [26].

Results

Figure 5 shows the CO and the AoP of a physiological circulation during the VM [panels (A) and (C)] and four PVCs [panels (B) and (D)]. The four phases of VM and the four PVCs are separated by dashed lines. After the onset of VM (phase 1) and a sudden AoP increase due to the increase of the ITP, the AoP decreased and made a trough during phase 2, while the CO decreased from 5 l/min to 2.5 l/min. In phase 3, at the end of VM, the AoP dropped suddenly together with the ITP. AoP recovered and increased up to 160 mm Hg. After a final oscillation, the AoP returned to its initial value. Accordingly, the CO increased up to approx. 7 l/min in phase 4 and then returned to 5 l/min.

During the PVCs, sudden CO drops can be observed, while the mean AoP decreased from 105 mm Hg to 90 mm Hg. After the last PVC both the CO and the AoP increased slightly above their initial values (end of phase 4) before they returned to their initial values ($t > 20$ s).

Figure 6 shows the effect of VM (left-hand side) and PVCs (right-hand side) on a pathological circulation assisted with a tVAD operated at a constant speed (C1). The figure shows the pump speed (PS) and flow (PF), the CO, the transmural pump inlet pressure (PIP) and the AoP. The PIP signal shows that suction (negative pressure) occurred during the VM. At the same time, the CO decreased and the AoP pulsatility was diminished. All signals recovered to the steady-state value after the end of the VM. During PVCs, all signals except the pump speed showed strong oscillations, but quickly returned to their steady-state values after the last PVC.

Figure 7 shows the effect of the VM and PVCs on a pathological circulation assisted with a tVAD controlled by the nominal PRS controller (C2). During the VM, due to the reduced LVV, the controller reduced the pump speed down to its minimum value of 1800 rpm at $t = 12$ s. The pump flow decreased as well as back flow occurred, while the CO decreased down to 1.5 l/min. The PIP signal shows that no suction occurred, while the mean AoP dropped down to approx. 60 mm Hg. During PVCs, the PS slowly adapted to the decreased LVV resulting from the arrhythmic beats. After the end of PVCs, the increased LV feeling led to a PS increase until it returned to a steady state. The mean PF, CO and AoP fluctuated according to the PS variations.

Figure 8 shows the effect of the VM and PVCs on a pathological circulation assisted with a tVAD controlled by the modified PRS controller (C3). In this case, the PS adaptation during the VM led to a minimum value of approx. 2500 rpm at $t = 12$ s. The PF decreased as well, but now back flow occurred. The minimum CO observed is 2.5 l/min. The maximum PIP dropped down to approx. 60 mm Hg and the mean AoP down to 80 mm Hg. A further AoP drop down to 60 mm Hg occurred after the end of VM. The PS adapted to the PVCs by decreasing the speed, whereas it increased during the normal contractions ($8 \text{ s} < t < 12.5$ s). Pump flow, CO and AoP varied similarly to PS.

Figure 9 shows the performance of the EDV detection methods for the configurations C2 and C3 during the experiments. An LVV decrease occurred during the VM [Figure 9 – panels (A) and (C)]. Clearly, the EDV detection algorithm of C2 shows a delayed detection during the LVV decrease compared to C3, which detected the EDV accurately at every beat. Panels (B) and (D) in Figure 9 show the irregular LVV waveform during the PVCs. The C3 configuration detected not only the EDV of the normal contraction but also the maximum volume during the premature ventricular contraction. Due to the 3 s moving window, the C2 configuration did not capture the sudden EDV drops during PVCs.

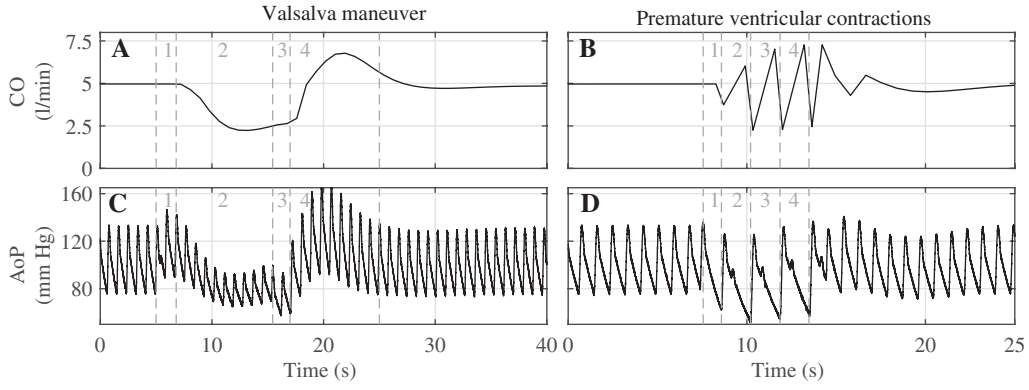

Figure 5: Cardiac output (CO) and aortic pressure (AoP) signals of a physiological circulation during the simulated Valsalva maneuver (VM) and premature ventricular contractions (PVCs). VM (A) and (C) and four PVCs (B) and (D).
Dashed lines indicate the four phases of the VM and the four PVCs.

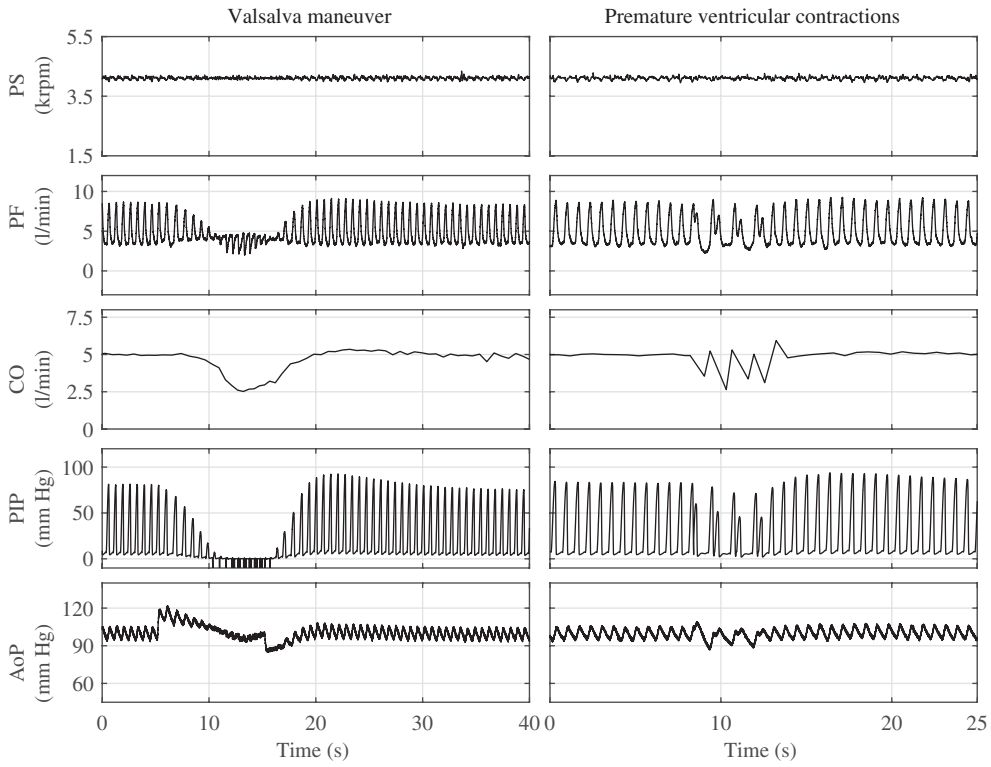

Figure 6: Performance of a pathological circulation assisted by a tVAD operated at a constant speed (C1) during the Valsalva maneuver (VM) (left-hand side panels) and premature ventricular contractions (PVCs) (right-hand side panels).
PS, Pump speed; PF, pump flow; CO, cardiac output; PIP, pump inlet pressure; AoP, aortic pressure.

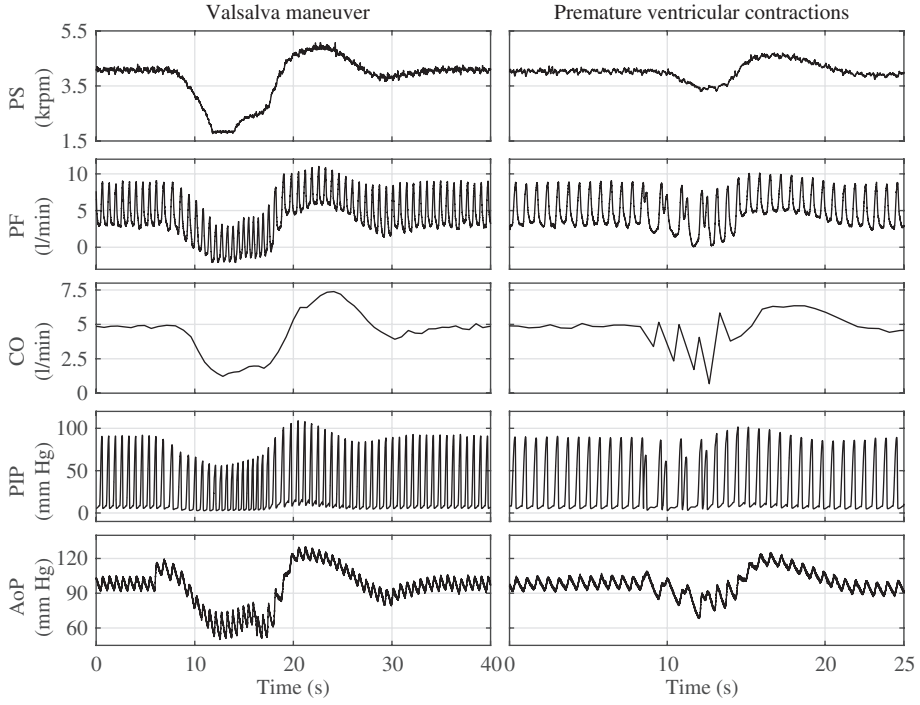

Figure 7: Performance of a pathological circulation assisted by a tVAD controlled by the nominal PRS controller (C2) during the Valsalva maneuver (left-hand side panels) and premature ventricular contractions (right-hand side panels).
PS, Pump speed; PF, pump flow; CO, cardiac output; PIP, pump inlet pressure; AoP, aortic pressure.

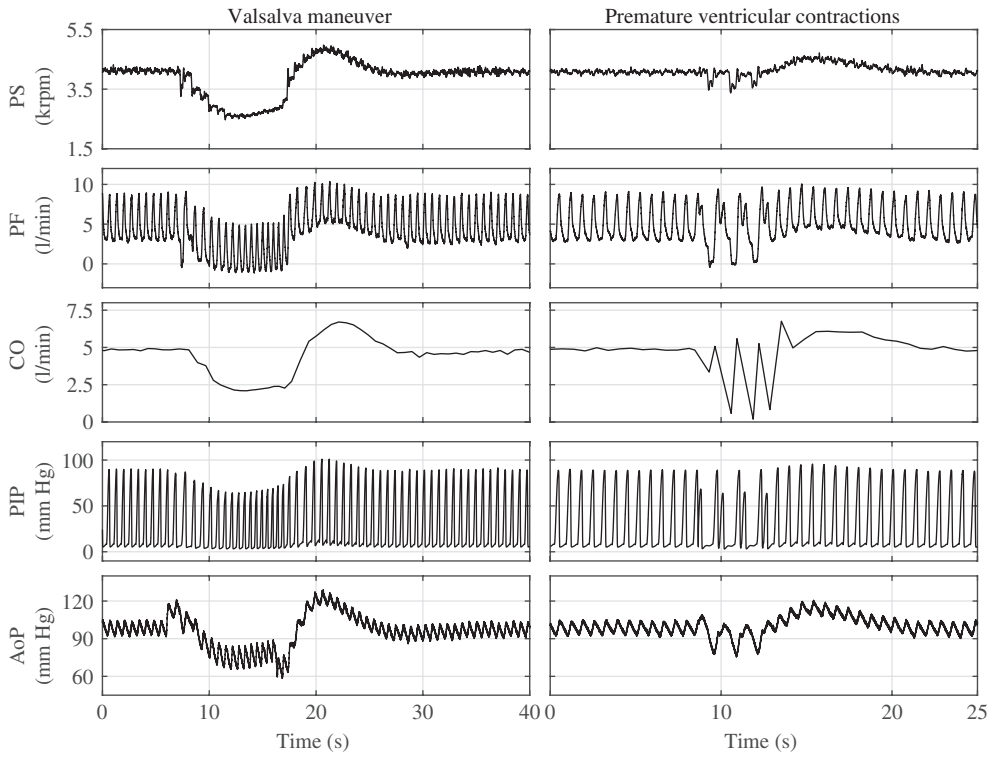

Figure 8: Performance of a pathological circulation assisted by a tVAD controlled by the modified PRS controller (C3) during the Valsalva maneuver (left-hand side panels) and premature ventricular contractions (right-hand side panels).
PS, Pump speed; PF, pump flow; CO, cardiac output; PIP, pump inlet pressure; AoP, aortic pressure.

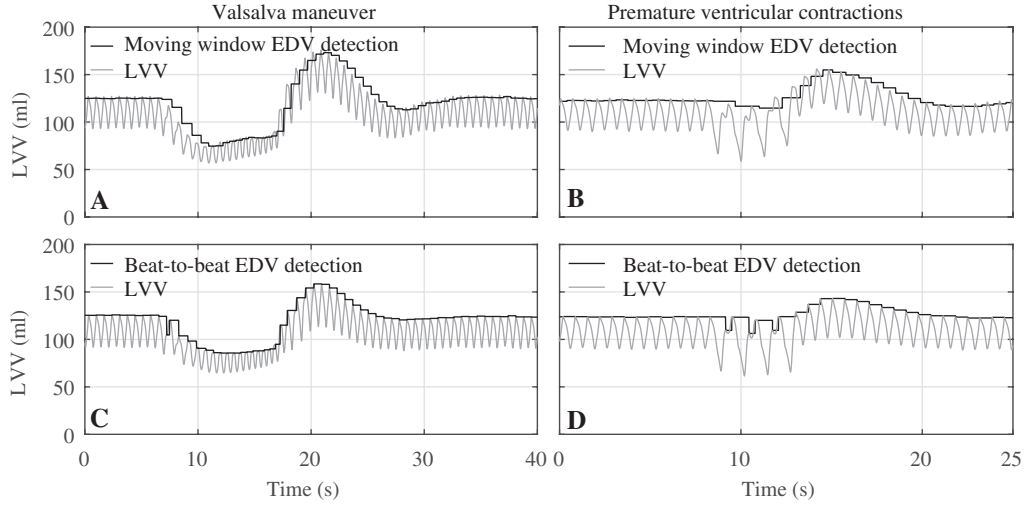

Figure 9: Comparison of two algorithms to extract the end-diastolic volume (EDV) from the left ventricular volume (LVV) signal during Valsalva maneuver [panels (A) and C)] and premature ventricular contractions [panels (B) and (D)].
Panels (A) and (B) show the performance of the 3-s moving window extraction algorithm used in C2. Panels (B) and (D) show the performance of the beat-to-beat EDV extraction algorithm used in C3.

Discussion

In this study, we investigated special patho-physiological situations that can lead to sudden changes of the venous return and therefore, suction or LV overloading. We simulated the VM on our HMC by introducing a change in the ITP. We increased the ITP to 30 mm Hg over 10 s, as it is reported from clinical experiments [8, 19, 29]. Such an

ITP increase can also occur during daily strain conditions of the patients, such as bowel movement, heavy lifting, coughing and posture changes [13]. The observed AoP signals of the physiological heart matched well with those reported in studies about clinical experiments [13, 29]. The four phases of VM seen in clinical recordings of arterial blood pressure were identified (Figure 5).

In the failing circulation without tVAD, a square-wave AoP response would be expected during the VM due to the blood pooling in the congested pulmonary vascular system, i.e. due to sustained LV preload [19, 29]. This was not observed in our experiments with the controlled tVAD support, where the AoP waveform during the VM was similar to that observed in the physiological circulation. This was to be expected, because the pulmonary vascular system was not congested in this case.

PVCs were simulated as described in [2], where the simulated results were validated based on the MIT-BIH arrhythmia database [10]. The moving window method detected the gradual LVV decrease resulting from the consecutive PVCs (Figure 7), while the beat-to-beat method was able to capture the sudden LVV changes between the irregular beats (Figure 8). No suction occurred during PVCs with neither of the configurations C1, C2, or C3. The case of sustained tachycardia was not included in our experiments, because we focused on the detection of abrupt and temporary hemodynamic changes.

The goal of this study was to investigate whether a beat-to-beat extraction of the EDV is required for a clinical physiological controller, or if a simpler method with a moving window is sufficient. We used the PRS controller [26] as a test controller. As it was developed in our group, we could faithfully configure and implement it. However, the results allow drawing conclusions for other physiological controllers, which rely on a certain feature that is extracted from the signal. The controllers presented in [1, 3, 6, 15, 21, 22, 26, 33] all use one of the two approaches investigated in the current study. Additionally, the presented numerical model can be a useful tool while tuning physiological controllers or defining their sampling rate, as such factors influence the aggressiveness of its response.

For our study, the lack of an implantable, long-term LV volume sensor is not addressed. We acknowledge the use of admittance catheters or sonomicrometry as a short-term, real time volume measurement for *in vivo* research studies, but these technologies are not suitable to be used in patients for long term. In the clinic, echocardiography or magnetic resonance imaging systems are normally used for the measurement of EDV, but they require computationally expensive post processing. In our group, we focus on the development of an implantable LV volume sensor that will be suitable for clinical applications.

The constant speed operation (C1) and the nominal PRS physiological controller (C2) were compared during the VM and the PVCs (Figures 6 and 7). The C2 configuration led to a pump speed and flow decrease during PVCs, which in turn decreased CO and AoP. After the end of the PVCs, a slight overshoot of all signals occurred due to the abrupt venous return recovery. This overshoot was absent in the case of C1 and the CO and AoP changes resembled better the physiological ones (Figure 5). During the VM, the physiological controller (C2) was able to prevent suction, whereas suction was observed with the constant speed (C1). The pump speed and flow adaptation of C2 led to stronger reduction of the CO during the VM, which is more physiological, but leads to a critically low AoP. The AoP waveform during constant speed operation resembled more that of a pathological circulation as presented in [19, 29], where the overshoot is attenuated.

Two different methods for extracting the index of the PRS controller were evaluated (C2 and C3). Both configurations performed better than the constant speed operation (C1) with respect to suction prevention. C3 outperformed C2 due to its faster response resulting from the beat-to-beat detection. The moving window of C2 introduced a delay (Figure 9). Comparing signals during VM between Figures 7 and 8, it is well visible that with C2, there was a greater drop in pump speed (lower speed limit was reached) than with C3. This lower speed resulted in turn in lower pump flow and CO. Backflow through the pump was higher with C2, thereby presumably increasing the probability for blood damage and thrombus formation due to blood recirculation and stagnation zones [4]. Furthermore, the lower pump flow with C2 led to lower AoP. Such low AoP may cause organ dysfunction and affect the quality of life of the patient. Thus, C2 led to less physiological hemodynamics compared to C3. With C1, the AoP sustained in physiological limits, but suction occurred. These outcomes show that the aggressiveness of a physiological controller may be hard to be identified when aiming to design an optimal controller. Additional algorithms to monitor parallel cases of suction, backflow, low AoP and adaptation of the response of the core physiological controller seems to be required for a better performance of a physiological controller.

During the PVCs with C3, the LVV dropped due to the additional contraction of the heart and the shortened diastolic phase. Thus, sudden speed changes occurred (Figure 8). Disturbances of the measured signal can lead to misdetection of the EDV with a beat-to-beat algorithm and therefore, undesirable speed changes. Furthermore,

such an extraction algorithm is considered to be more complex thus increasing the sensitivity to measurement noise, the probability for wrong feature extraction and ultimately reducing the stability margins of the controller in a clinical implementation. On the other hand, a moving window algorithm is considered quite simple, robust and independent of the HR of the native heart. However, the lack of fast adaptation to short-time acute events can lead to momentarily high flows during premature contractions and intermittent suction events or strong maneuvers. Considering all these results, a trade-off is observed between a fast response, which can more likely prevent overpumping and underpumping and a slower response, which is more robust. For a clinical implementation, robustness should be the major goal.

One direct impact of physiological control could be the avoidance of low-flow alarms, which occur frequently in clinical practice. They directly affect the workload of the clinical staff and thus increase treatment costs. Typical everyday activities like coughing, bowel movement, heavy lifting, sleep apnea or even deep breathing can affect ITP and lead to abrupt blood flow changes. With physiological control, the pump flow will be adapted to such activities and the risks of overpumping and underpumping events can be reduced drastically. The clinical routines for monitoring VAD-patients would need to be revised, as low-flows will, hopefully, not constitute such a critical condition for the patients any more. This can also contribute to reduce the psychological stress of the patients and thus improve their quality of life as well as the workload of the health care professionals. However, the development of physiological controller that can achieve all this positive impact constitutes a multi-objective task. It seems that a very fast suction prevention may result to non-physiological hemodynamics, thus reducing the positive effect of a controller. Therefore, the statement that a physiological controller is superior to constant speed should be carefully stated and the comparison between them should be based on realistic, clinically frequent scenarios.

The development of a tVAD and its regulatory approval require extensive *in vivo* testing. Because these tests are expensive and ethically problematic, it is very important to gain as much knowledge as possible from *in vitro* tests. Therefore, it is important to test physiological controllers against all possible patho-physiological events that may occur and thereby influence the performance of the controller. With our extended numerical model of the human blood circulation, we propose an additional tool for testing physiological controllers that can contribute to boost the trust in *in vitro* testing and thus reduce the amount required in *in vivo* trials.

Funding: The authors gratefully acknowledge the financial support by the Stavros Niarchos Foundation. This work is part of the Zurich Heart project under the umbrella of "University Medicine Zurich".
Conflict of interest: The authors declare no conflict of interest.

References

[1] AlOmari AHH, Savkin AV, Stevens M, et al. Developments in control systems for rotary left ventricular assist devices for heart failure patients: a review. Physiol Meas 2013; 34: R1–R27.
[2] Amacher R, Ochsner G, Ferreira A, Vandenberghe S, Schmid Daners M. A robust reference signal generator for synchronized ventricular assist devices. IEEE Trans Biomed Eng 2013; 60: 2174–2183. ISSN 1558-2531.
[3] Arndt A, Nüsser P, Lampe B, Müller J. Physiological control of a rotary left ventricular assist device: robust control of pressure pulsatility with suction prevention and suppression. In: World Congress on Medical Physics and Biomedical Engineering, Munich, Germany, Volume 25/7. IFMBE Proceedings, September 7–12. Berlin Heidelberg: Springer, 2009. pp. 775–778.
[4] Behbahani M, Behr M, Hormes M, et al. A review of computational fluid dynamics analysis of blood pumps. Eur J Appl Math 2009; 20: 363.
[5] Bergan JJ, Bunke-Paquette N. The vein book. Oxford: Oxford University Press 2014.
[6] Bullister E, Reich S, Sluetz J. Physiologic control algorithms for rotary blood pumps using pressure sensor input. Artif Organs 2002; 26: 931–938.
[7] Colacino FM, Moscato F, Piedimonte F, Arabia M, Danieli GA. Left ventricle load impedance control by apical vad can help heart recovery and patient perfusion: a numerical study. ASAIO J 2007; 53: 263–277.
[8] Felker GM, Cuculich PS, Gheorghiade M. The valsalva maneuver: a bedside "biomarker" for heart failure. Am J Med 2006; 119: 117–122.
[9] Gaddum NR, Stevens M, Lim E, et al. Starling-like flow control of a left ventricular assist device: *in vitro* validation. Artif Organs 2014; 38: E46–E56.
[10] Goldberger AL, Amaral LA, Glass L, et al. Physiobank, physiotoolkit, and physionet components of a new research resource for complex physiologic signals. Circulation 2000; 101: e215–e220.
[11] Hall JE, Guyton AC. Textbook of medical physiology. London: Saunders 2011.
[12] Kirklin JK, Naftel DC, Pagani FD, et al. Seventh intermacs annual report: 15,000 patients and counting. J Heart Lung Transplant 2015; 34 :1495–1504.
[13] Klabunde R. Cardiovascular physiology concepts. Baltimore, MD, USA: Lippincott Williams & Wilkins 2011.
[14] Liang F, Liu H. Simulation of hemodynamic responses to the valsalva maneuver: an integrative computational model of the cardiovascular system and the autonomic nervous system. J Physiol Sci 2006; 56: 45–65.

[15] Lim ET, Alomari AH, Savkin AV, et al. A method for control of an implantable rotary blood pump for heart failure patients using noninvasive measurements. Artif Organs 2011; 35: E174–E180.
[16] Lim E, Chan GS, Dokos S, et al. A cardiovascular mathematical model of graded head-up tilt. PLoS One 2013; 8: e77357.
[17] Lim E, Dokos S, Cloherty SL, et al. Parameter-optimized model of cardiovascular-rotary blood pump interactions. IEEE Trans Biomed Eng 2010; 57: 254–266.
[18] Lim E, Salamonsen RF, Mansouri M, et al. Hemodynamic response to exercise and head-up tilt of patients implanted with a rotary blood pump: a computational modeling study. Artif Organs 2015; 39: E24–E35.
[19] Little WC, Barr WK, Crawford MH. Altered effect of the valsalva maneuver on left ventricular volume in patients with cardiomyopathy. Circulation 1985; 71: 227–233.
[20] MacDougall J, McKelvie R, Moroz D, Sale D, McCartney N, Buick F. Factors affecting blood pressure during heavy weight lifting and static contractions. J Appl Physiol 1992; 73: 1590–1597.
[21] Mansouri M, Salamonsen RF, Lim E, Akmeliawati R, Lovell NH. Preload-based starling-like control for rotary blood pumps: numerical comparison with pulsatility control and constant speed operation. PLoS One 2015; 10: e0121413. ISSN 1932-6203.
[22] Moscato F, Arabia M, Colacino FM, Naiyanetr P, Danieli GA, Schima H. Left ventricle after load impedance control by an axial flow ventricular assist device: a potential tool for ventricular recovery. Artif Organs 2010; 34: 736–744.
[23] Moscato F, Arabia M, Naiyanetr P, Danieli G, Schima H. Control of a rotary blood pump for defined ventricular unloading: a potential tool for ventricular recovery. In: World Congress on Medical Physics and Biomedical Engineering. Munich, Germany, Volume 25/7. IFMBE Proceedings, September 7–12, 2009. Berlin Heidelberg: Springer, pp. 502–505.
[24] Ochsner G, Amacher R, Amstutz A, et al. A novel interface for hybrid mock circulations to evaluate ventricular assist devices. IEEE Trans Biomed Eng 2013; 60: 507–516. ISSN 1558-2531.
[25] Ochsner G, Amacher R, Schmid Daners M. Emulation of ventricular suction in a hybrid mock circulation. In: Proceedings of the 12th European Control Conference, New York City, NY, USA 2013. pp. 3108–3112.
[26] Ochsner G, Amacher R, Wilhelm MJ, et al. A physiological controller for turbodynamic ventricular assist devices based on a measurement of the left ventricular volume. Artif Organs 2013; 38: 527–538. ISSN 0160-564X.
[27] Samet P. Hemodynamic sequelae of cardiac arrhythmias. Circulation 1973; 47: 399–407.
[28] Schumer EM, Ising MS, Slaughter MS. The current state of left ventricular assist devices: challenges facing further development. Expert Rev Cardiovasc Ther 2015; 13: 1–9.
[29] Sharpey-Schafer E. Effects of valsalva's manoeuvre on the normal and failing circulation. Br Med J 1955; 1: 693.
[30] Stevens MC, Wilson S, Bradley A, Fraser J, Timms D. Physiological control of dual rotary pumps as a biventricular assist device using a master/slave approach. Artif Organs 2014; 38: 766–774.
[31] Ten Harkel A, Van Lieshout J, Van Lieshout E, Wieling W. Assessment of cardiovascular reflexes: influence of posture and period of preceding rest. J Appl Physiol 1990; 68: 147–153.
[32] Timms DL, Gregory SD, Stevens MC, Fraser JF. Haemodynamic modeling of the cardiovascular system using mock circulation loops to test cardiovascular devices. In: Engineering in Medicine and Biology Society, EMBC, 2011 Annual International Conference of the IEEE. New York City, NY, USA: IEEE, 2011. pp. 4301–4304.
[33] Wang Y, Koenig SC, Slaughter MS, Giridharan GA. Rotary blood pump control strategy for preventing left ventricular suction. ASAIO J 2015; 61: 21–30.
[34] Xie A, Phan K, Yan TD. Durability of continuous-flow left ventricular assist devices: a systematic review. Ann Thorac Surg 2014; 3: 547.